

**NASA
Technical
Paper
2725**

August 1987

Comparison of Theoretical and
Experimental Thrust Performance
of a 1030:1 Area Ratio Rocket
Nozzle at a Chamber Pressure
of 2413 kN/m² (350 psia)

Tamara A. Smith,
Albert J. Pavli, and
Kenneth J. Kacynski

NASA

**NASA
Technical
Paper
2725**

1987

Comparison of Theoretical and
Experimental Thrust Performance
of a 1030:1 Area Ratio Rocket
Nozzle at a Chamber Pressure
of 2413 kN/m² (350 psia)

Tamara A. Smith,
Albert J. Pavli, and
Kenneth J. Kacynski

*Lewis Research Center
Cleveland, Ohio*



National Aeronautics
and Space Administration

Scientific and Technical
Information Office

Summary

The Joint Army, Navy, NASA, Air Force (JANNAF) rocket engine performance prediction procedure is based on the use of various reference computer programs. One of the reference programs for nozzle analysis is the Two-Dimensional Kinetics (TDK) Program. The purpose of this report is to calibrate the JANNAF procedure that has been incorporated into the December 1984 version of the TDK program for the high-area-ratio rocket engine regime. The calibration was accomplished by modeling the performance of a 1030:1 rocket nozzle tested at NASA Lewis Research Center. A detailed description of the test conditions and TDK input parameters is given.

The results indicate that the computer code predicts delivered vacuum specific impulse to within 0.12 to 1.9 percent of the experimental data. Vacuum thrust coefficient predictions were within ± 1.3 percent of experimental results. Predictions of wall static pressure were within approximately ± 5 percent of the measured values. An experimental value for inviscid thrust was obtained for the nozzle extension between area ratios of 427.5 and 1030 by using an integration of the measured wall static pressures. Subtracting the measured thrust gain produced by the nozzle between area ratios of 427.5 and 1030 from the inviscid thrust gain yielded experimental drag decrements of 10.85 and 27.00 N (2.44 and 6.07 lb) for mixture ratios of 3.04 and 4.29, respectively. These values correspond to 0.45 and 1.11 percent of the total vacuum thrust. At a mixture ratio of 4.29, the TDK predicted drag decrement was 16.59 N (3.73 lb), or 0.71 percent of the predicted total vacuum thrust.

Introduction

In 1975, the Joint Army, Navy, NASA, Air Force (JANNAF) Rocket Engine Performance Working Group developed and documented a methodology to model rocket engine systems. This methodology, outlined in reference 1, was developed to create an industry and government reference for rocket engine performance prediction.

The JANNAF prediction procedure makes use of various reference computer programs. One of the reference programs is the Two-Dimensional Kinetics (TDK) Program for nozzle analysis (ref. 2). TDK was originally developed under the auspices of the JANNAF working group. At that time, TDK

performed a two-dimensional, inviscid calculation of rocket nozzle performance. Over the years, the TDK program has been extended to include a prediction of viscous effects on nozzle performance using the JANNAF procedure.

When the JANNAF procedure was developed, large-area-ratio rocket nozzles extended to area ratios of 100. With the recent effort to develop engines for applications such as the orbital transfer vehicle, rocket nozzle designs with area ratios of 1000 or larger are being examined. Because these high-area-ratio nozzles create a new performance prediction domain, it is unclear how well the JANNAF procedure will predict. Therefore, there is a need to calibrate the procedure for this rocket engine regime.

The purpose of this report is to calibrate the JANNAF procedure that was incorporated into the December 1984 version of the TDK program. The calibration is accomplished by modeling the performance of a 1030:1 rocket nozzle tested at NASA Lewis Research Center. A detailed description of the test conditions and TDK input parameters is given.

This report presents experimental vacuum thrust and vacuum specific impulse $I_{sp,v}$ data for an optimally contoured nozzle, which was extended to an exit area ratio of 1030 and could be truncated to an exit area ratio of 427.5. The nozzle was tested using a gaseous hydrogen and gaseous oxygen combustion system at a nominal chamber pressure of 2413 kN/m² (350 psia) and a propellant mixture ratio O/F range of 2.78 to 5.49 (ref. 3). The experimental thrust and $I_{sp,v}$ results are compared to the theoretical predictions obtained from the TDK computer code.

Experimental wall static pressures were used to quantify the inviscid thrust gain between the area ratios of 427.5 and 1030. By comparing this inviscid thrust to the measured thrust gain, we obtained a value for the shear (or drag) force. Corresponding values were obtained from the TDK program and compared to the experimental results.

Background

Test Facility

Testing was done in the new altitude test capsule at the NASA Lewis Rocket Engine Test Facility (RETF). Figure 1 is an illustration of RETF with cutaway views of the test capsule and spray cooler. The operation of the facility was

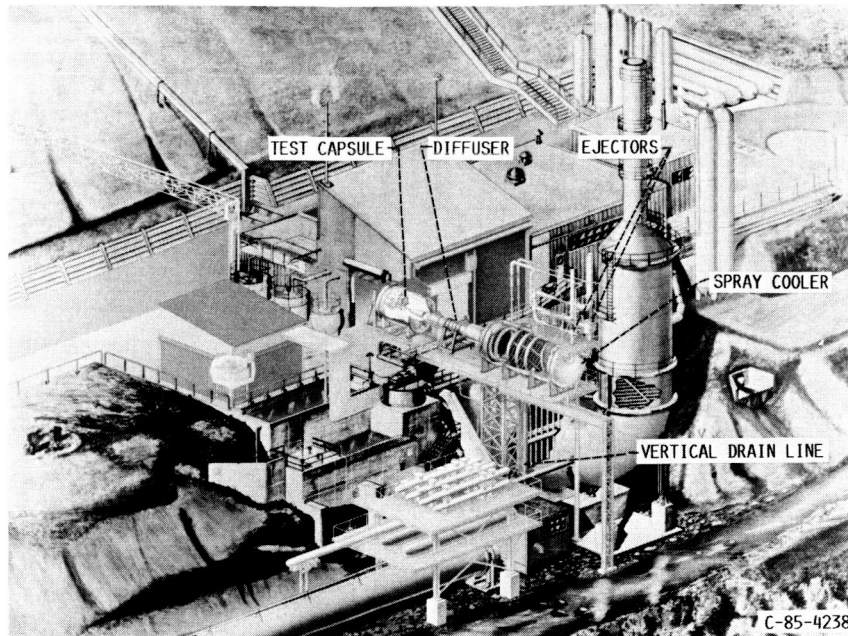


Figure 1.—Rocket Engine Test Facility (RETF) with cutaway views of test capsule and spray cooler.

as follows. When the engine was fired, the exhaust gases flowed into the diffuser where the kinetic energy of the exhaust was used to accomplish some of the altitude pumping. From the diffuser, the exhaust gases flowed into the spray cooler, where approximately one-half of the exhaust was condensed to water and flowed out the vertical drain line. The other half was pumped by the gaseous nitrogen ejectors shown mounted on top of the spray cooler. The pressure obtained in the test capsule was in the range of 0.207 to 0.34 kN/m² (0.03 to

0.05 psia). A more indepth description of the facility and test apparatus can be found in reference 3.

The thrust stand used in this facility was capable of measuring 13.34 kN (3000 lb) full scale and was attached to a foundation that was separate from the test capsule bulkhead. The thrust stand was designed to have a 2σ (standard deviation) variation of less than ± 0.1 percent of full scale, and it was calibrated against a load cell that had a 2σ variation of less than ± 0.05 percent of full scale.

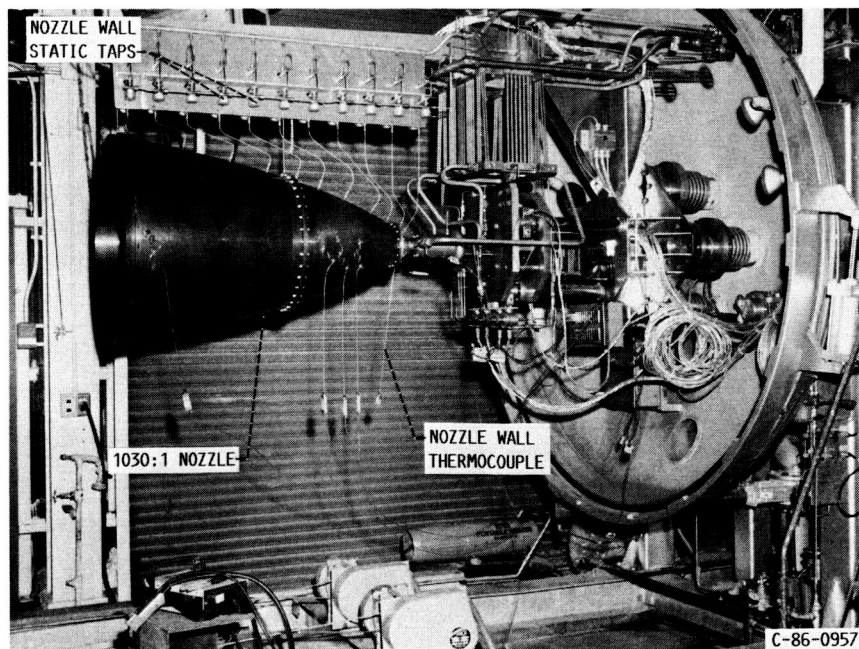


Figure 2.—Altitude test capsule—1030:1 nozzle being installed in thrust stand.

Test Hardware

Figure 2, which is a photograph of the inside of the test capsule, shows the thrust stand with the 1030:1 nozzle in the process of being installed. The injector used during these tests had 36 gaseous oxygen shower-head elements, with the gaseous hydrogen flowing through a porous face plate. The solid copper combustion chamber was 15.24 cm (6 in.) long and had an inside diameter of 5.2197 cm (2.055 in.). It was uncooled (heat-sink) hardware that relied on its thermal capacitance to survive the short firings (<3 sec).

The 1030:1 nozzle was made of three sections. The first, the throat section, connected to the combustion chamber, converged to the 2.54 cm (1 in.) throat, and then diverged to an area ratio of 29.9. The throat section was made of nickel with a ceramic coating on the inner wall and had a water jacket around the throat that extended to an area ratio of approximately 5. The next section of the nozzle expanded to an area ratio of 427.5 and was made of 0.635 cm (0.25 in.) carbon steel. The last section of the nozzle extended to an area ratio of 1030 and was also made of 0.635-cm (0.25-in.) carbon steel. The carbon steel sections were heat-sink hardware and had no ceramic coatings.

The 1030:1 nozzle contour was designed using the Rao Nozzle Contour Program (ref. 4) and the Boundary-Layer Integral Matrix Procedure (BLIMP-J) (ref. 5) program. The Rao program provided the inviscid optimal nozzle contour, and the BLIMP-J program estimated the boundary-layer displacement thickness along the nozzle. The combination of the two results provided the nozzle coordinates that were used to make the hardware. Figure 3 shows the nozzle contour and coordinates. A further discussion of the nozzle design is presented in reference 3.

Analysis

The TDK computer program evaluates the two-dimensional nonequilibrium chemistry and viscous effects on the performance of rocket exhaust nozzles. Version 2.4 (December 1984) of TDK was used in this report. TDK consists of a master control module (MCM) and five computational modules: ODE, ODK, TRAN, MOC, and BLM. The MCM controls the execution of TDK and processes the output.

The ODE (one-dimensional equilibrium) module calculates ideal engine performance assuming either chemical equilibrium composition or a frozen chemical composition at rocket chamber conditions. ODE uses the free-energy minimization method to compute equilibrium conditions for any assigned enthalpy and pressure.

The ODK (one-dimensional kinetics) module calculates the inviscid, one-dimensional nonequilibrium nozzle expansion of gaseous propellant exhaust.

The TRAN (transonic flow) module uses the chemical information computed by ODK to estimate two-dimensional effects in the transonic region of the nozzle throat. The purpose of these calculations is to approximate an initial data line across

the nozzle throat in order to start the method of characteristics (MOC) calculations.

The MOC module uses the method of characteristics to construct a finite-difference mesh by tracing gas streamlines and characteristic surfaces. By determining the properties of the exhaust at the mesh points, MOC is able to calculate the loss in nozzle performance caused by flow divergence.

The BLM (boundary-layer module) calculates compressible laminar and turbulent wall boundary layers in axisymmetric nozzles. BLM uses the two-point finite-difference method developed by Keller and Cebeci (ref. 6) to calculate the boundary-layer properties and Cebeci-Smith eddy-viscosity formulation (ref. 7) to model the turbulent boundary layer.

The experimental hardware specifications and test conditions were used to write the input files to TDK so that this program could accurately model the nozzle performance. The input variables that described the nozzle inlet geometry are listed in table I. The nozzle contour coordinates that were used are shown in figure 3. Table II shows the experimental results that were also used in the TDK input files: effective chamber

NOZZLE COORDINATES			
AXIAL DISTANCE FROM THROAT		RADIUS	
cm	in.	cm	in.
0.0000	0.0000	1.2700	0.5000
.3929	.1547	1.4371	.5658
.7858	.3094	1.6042	.6316
1.1787	.4641	1.7713	.6974
1.5716	.6188	1.9384	.7632
1.9645	.7735	2.1055	.8290
2.3574	.9282	2.2726	.8948
2.7503	1.0829	2.4397	.9606
3.1432	1.2376	2.6068	1.0264
3.5361	1.3923	2.7739	1.0922
3.9290	1.5470	2.9410	1.1580
4.3219	1.7017	3.1081	1.2238
4.7148	1.8564	3.2752	1.2896
5.1077	2.0111	3.4423	1.3554
5.5006	2.1658	3.6094	1.4212
5.8935	2.3205	3.7765	1.4870
6.2864	2.4752	3.9436	1.5528
6.6793	2.6299	4.1107	1.6186
7.0722	2.7846	4.2778	1.6844
7.4651	2.9393	4.4449	1.7502
7.8580	3.0940	4.6120	1.8160
8.2509	3.2487	4.7791	1.8818
8.6438	3.4034	4.9462	1.9476
9.0367	3.5581	5.1133	2.0134
9.4296	3.7128	5.2804	2.0792
9.8225	3.8675	5.4475	2.1450
10.2154	4.0222	5.6146	2.2108
10.6083	4.1769	5.7817	2.2766
11.0012	4.3316	5.9488	2.3424
11.3941	4.4863	6.1159	2.4082
11.7870	4.6410	6.2830	2.4740
12.1800	4.7957	6.4501	2.5398
12.5729	4.9504	6.6172	2.6056
12.9658	5.1051	6.7843	2.6714
13.3587	5.2598	6.9514	2.7372
13.7516	5.4145	7.1185	2.8030
14.1445	5.5692	7.2856	2.8688
14.5374	5.7239	7.4527	2.9346
14.9303	5.8786	7.6198	3.0004
15.3232	6.0333	7.7869	3.0662
15.7161	6.1880	7.9540	3.1320
16.1090	6.3427	8.1211	3.1978
16.5019	6.4974	8.2882	3.2636
16.8948	6.6521	8.4553	3.3294
17.2877	6.8068	8.6224	3.3952
17.6806	6.9615	8.7895	3.4610
18.0735	7.1162	8.9566	3.5268
18.4664	7.2709	9.1237	3.5926
18.8593	7.4256	9.2908	3.6584
19.2522	7.5803	9.4579	3.7242
19.6451	7.7350	9.6250	3.7900
20.0380	7.8897	9.7921	3.8558
20.4309	8.0444	9.9592	3.9216
20.8238	8.1991	10.1263	3.9874
21.2167	8.3538	10.2934	4.0532
21.6096	8.5085	10.4605	4.1190
22.0025	8.6632	10.6276	4.1848
22.3954	8.8179	10.7947	4.2506
22.7883	8.9726	10.9618	4.3164
23.1812	9.1273	11.1289	4.3822
23.5741	9.2820	11.2960	4.4480
23.9670	9.4367	11.4631	4.5138
24.3600	9.5914	11.6302	4.5796
24.7529	9.7461	11.7973	4.6454
25.1458	9.9008	11.9644	4.7112
25.5387	10.0555	12.1315	4.7770
25.9316	10.2102	12.2986	4.8428
26.3245	10.3649	12.4657	4.9086
26.7174	10.5196	12.6328	4.9744
27.1103	10.6743	12.8000	5.0402
27.5032	10.8290	12.9671	5.1060
27.8961	10.9837	13.1342	5.1718
28.2890	11.1384	13.3013	5.2376
28.6819	11.2931	13.4684	5.3034
29.0748	11.4478	13.6355	5.3692
29.4677	11.6025	13.8026	5.4350
29.8606	11.7572	13.9697	5.5008
30.2535	11.9119	14.1368	5.5666
30.6464	12.0666	14.3039	5.6324
31.0393	12.2213	14.4710	5.6982
31.4322	12.3760	14.6381	5.7640
31.8251	12.5307	14.8052	5.8298
32.2180	12.6854	14.9723	5.8956
32.6109	12.8401	15.1394	5.9614
33.0038	12.9948	15.3065	6.0272
33.3967	13.1495	15.4736	6.0930
33.7896	13.3042	15.6407	6.1588
34.1825	13.4589	15.8078	6.2246
34.5754	13.6136	15.9749	6.2904
34.9683	13.7683	16.1420	6.3562
35.3612	13.9230	16.3091	6.4220
35.7541	14.0777	16.4762	6.4878
36.1470	14.2324	16.6433	6.5536
36.5400	14.3871	16.8104	6.6194
36.9329	14.5418	16.9775	6.6852
37.3258	14.6965	17.1446	6.7510
37.7187	14.8512	17.3117	6.8168
38.1116	15.0059	17.4788	6.8826
38.5045	15.1606	17.6459	6.9484
38.8974	15.3153	17.8130	7.0142
39.2903	15.4700	17.9801	7.0800
39.6832	15.6247	18.1472	7.1458
40.0761	15.7794	18.3143	7.2116
40.4690	15.9341	18.4814	7.2774
40.8619	16.0888	18.6485	7.3432
41.2548	16.2435	18.8156	7.4090
41.6477	16.3982	18.9827	7.4748
42.0406	16.5529	19.1498	7.5406
42.4335	16.7076	19.3169	7.6064
42.8264	16.8623	19.4840	7.6722
43.2193	17.0170	19.6511	7.7380
43.6122	17.1717	19.8182	7.8038
44.0051	17.3264	19.9853	7.8696
44.3980	17.4811	20.1524	7.9354
44.7909	17.6358	20.3195	8.0012
45.1838	17.7905	20.4866	8.0670
45.5767	17.9452	20.6537	8.1328
45.9696	18.1000	20.8208	8.1986
46.3625	18.2547	20.9879	8.2644
46.7554	18.4094	21.1550	8.3302
47.1483	18.5641	21.3221	8.3960
47.5412	18.7188	21.4892	8.4618
47.9341	18.8735	21.6563	8.5276
48.3270	19.0282	21.8234	8.5934
48.7200	19.1829	21.9905	8.6592
49.1129	19.3376	22.1576	8.7250
49.5058	19.4923	22.3247	8.7908
49.8987	19.6470	22.4918	8.8566
50.2916	19.8017	22.6589	8.9224
50.6845	19.9564	22.8260	8.9882
51.0774	20.1111	22.9931	9.0540
51.4703	20.2658	23.1602	9.1198
51.8632	20.4205	23.3273	9.1856
52.2561	20.5752	23.4944	9.2514
52.6490	20.7299	23.6615	9.3172
53.0419	20.8846	23.8286	9.3830
53.4348	21.0393	23.9957	9.4488
53.8277	21.1940	24.1628	9.5146
54.2206	21.3487	24.3299	9.5804
54.6135	21.5034	24.4970	9.6462
55.0064	21.6581	24.6641	9.7120
55.3993	21.8128	24.8312	9.7778
55.7922	21.9675	24.9983	9.8436
56.1851	22.1222	25.1654	9.9094
56.5780	22.2769	25.3325	9.9752
56.9709	22.4316	25.4996	10.0410
57.3638	22.5863	25.6667	10.1068
57.7567	22.7410	25.8338	10.1726
58.1496	22.8957	25.9999	10.2384
58.5425	23.0504	26.1670	10.3042
58.9354	23.2051	26.3341	10.3700
59.3283	23.3598	26.5012	10.4358
59.7212	23.5145	26.6683	10.5016
60.1141	23.6692	26.8354	10.5674
60.5070	23.8239	27.0025	10.6332
60.9000	23.9786	27.1696	10.6990
61.2929	24.1333	27.3367	10.7648
61.6858	24.2880	27.5038	10.8306
62.0787	24.4427	27.6709	10.8964
62.4716	24.5974	27.8380	10.9622
62.8645	24.7521	28.0051	11.0280
63.2574	24.9068	28.1722	11.0938
63.6503	25.0615	28.3393	11.1596
64.0432	25.2162	28.5064	11.2254
64.4361	25.3709	28.6735	11.2912
64.8290	25.5256	28.8406	11.3570
65.2219	25.6803	29.0077	11.4228
65.6148	25.8350	29.1748	11.4886
66.0077	25.9897	29.3419	11.5544
66.4006	26.1444	29.5090	11.6202
66.7935	26.2991	29.6761	11.6860
67.1864	26.4538	29.8432	11.7518
67.5793	26.6085	30.0103	11.8176
67.9722	26.7632	30.1774	11.8834
68.3651	26.9179	30.3445	11.9492
68.7580	27.0726	30.5116	12.0150
69.1509	27.2273	30.6787	12.0808
69.5438	27.3820	30.8458	12.1466
69.9367	27.5367	31.0129	12.2124
70.3296	27.6914	31.1800	12.2782
70.7225	27.8461	31.3471	12.3440
71.1154	28.0008	31.5142	12.4098
71.5083	28.1555	31.6813	12.4756
71.9012	28.3102	31.8484	12.5414
72.2941	28.4649	32.0155	12.6072
72.6870	28.6196	32.1826	12.6730
73.0800	28.7743	32.3497	12.7388
73.4729	28.9290	32.5168	12.8046
73.8658	29.0837	32.6839	12.8704
74.2587	29.2384	32.8510	12.9362
74.6516	29.3931	33.0181	13.0020
75.0445	29.5478	33.1852	13.0678
75.4374	29.7025	33.3523	13.1336
75.8303	29.8572	33.5194	13.1994
76.2232	30.0119	33.6865	13.2652
76.6161	30.1666	33.8536	13.3310
77.0090	30.3213	34.0207	13.3968
77.4019	30.4760	34.1878	13.4626
77.7948	30.6307	34.3549	13.5284
78.1877	30.7854	34.5220	13.5942
78.5806	30.9401	34.6891	13.6600
78.9735	31.0948	34.8562	13.7258
79.3664	31.2495	35.0233	13.7916
79.7593	31.4042	35.1904	13.8574
80.1522	31.5589	35.3575	13.9232
80.5451	31.7136	35.5246	13.9890
80.9380	31.8683	35.6917	14.0548
81.3309	32.0230	35.8588	14.1206
81.7238	32.1777	36.0259	14.1864
82.1167	32.3324	36.1930	14.2522
82.5096	32.4871	36.3601	14.3180
82.9025	32.6418	36.5272</	

TABLE I.—TWO-DIMENSIONAL KINETICS (TDK) INPUT VARIABLES

Parameter	TDK variable	Value
Throat radius, cm (in.)	RSI	1.27(0.5)
Inlet contraction ratio	ECRAT	4.223
Inlet wall radius ^a	RI	2.0
Inlet angle, deg	THETA I	25.0
Upstream wall radius of curvature ^a	RWTU	2.0
Downstream wall radius of curvature ^a	RWTD	0.4
Nozzle attachment angle, deg	THETA	39.41
Nozzle exit angle, deg	THE	7.94 ^b

^aNormalized by throat radius.

^bTHE = 15.5 for truncated contour.

TABLE II.—EXPERIMENTAL RESULTS

Reading	Nozzle exit expansion area ratio, ϵ	Effective chamber pressure $P_{c,e}$		Propellant mixture ratio, O/F	Fuel injection pressure		Fuel injection temperature		Oxidizer injection pressure		Oxidizer injection temperature		Propellant flow rate		
		kN/m ²	psia		kN/m ²	psia	K	°R	kN/m ²	psia	K	°R	kg/sec	lb/sec	
112	1030 ↓ 427.5 427.5	2482	360.0	3.84	3061	444.0	285.6	514.1	2809	407.4	279.2	502.5	0.5266	1.161	
113		2461	356.9	4.36	2956	428.8	284.2	511.5	2818	408.7	277.0	498.6	.5334	1.176	
114		2488	360.9	5.08	2912	422.4	283.9	511.1	2890	419.2	275.8	496.4	.5543	1.222	
115		2450	355.3	5.49	2843	412.4	283.5	510.3	2870	416.3	275.9	496.6	.5552	1.224	
117		2456	356.2	3.19	3160	458.3	281.1	506.0	2735	396.7	275.1	495.2	.5094	1.123	
120		2449	355.2	4.30	2950	427.8	294.4	529.9	2803	406.6	287.5	517.5	.5316	1.172	
121		2482	360.0	4.11	3013	437.0	295.0	531.0	2832	410.7	288.3	518.9	.5293	1.167	
123		2449	355.2	3.19	3152	457.2	295.6	532.0	2732	396.2	289.4	521.0	.5039	1.111	
124		2492	361.4	2.78	3328	482.7	295.9	532.6	2752	399.1	289.5	521.1	.5058	1.115	
125		2441	354.0	3.74	3028	439.1	296.3	533.3	2763	400.7	289.2	520.6	.5135	1.132	
136		427.5	2383	345.6	3.04	3123	452.9	292.1	525.7	2648	384.1	287.6	517.7	.4917	1.084
137		427.5	2457	356.8	4.29	2965	430.0	291.2	524.2	2813	408.0	285.0	531.0	.5330	1.175

Reading	Vacuum thrust, F_V		Ambient pressure around nozzle, P_a		Characteristic exhaust velocity, C^*		Characteristic exhaust velocity efficiency, η_{C^*} , percent	Measured vacuum thrust coefficient, $C_{F,V}$	Vacuum thrust coefficient efficiency, $\eta_{C_{F,V}}$, percent	Vacuum specific impulse, $I_{sp,V}$, sec	Vacuum specific impulse efficiency, $\eta_{I_{sp,V}}$, percent
	N	lb	kN/m ²	psia	m/sec	ft/sec					
112	2422	544.4	0.2682	0.0389	2424	7953	96.4	1.917	97.3	468.9	92.9
113	2409	541.6	.2592	.0376	2366	7762	95.8	1.914	95.3	460.4	90.5
114	2457	552.3	.2530	.0367	2305	7562	95.3	1.941	94.0	451.9	88.8
115	2448	550.4	.2530	.0367	2261	7418	94.9	1.967	93.7	449.7	88.3
117	2364	531.5	.2461	.0357	2473	8115	97.2	1.892	98.4	473.4	94.9
120	2429	546.1	.2544	.0369	2382	7815	95.9	1.923	96.0	466.1	91.8
121	2459	552.9	.2654	.0385	2403	7885	96.2	1.921	96.6	473.6	93.5
123	2377	534.3	.2592	.0376	2477	8128	97.2	1.881	97.7	481.1	96.2
124	2336	536.4	.2441	.0354	2502	8208	97.8	1.857	97.8	481.3	97.3
125	2406	541.0	.2420	.0351	2433	7984	96.5	1.912	97.4	477.8	94.6
136	2228	500.9	.3916	.0568	2487	8158	97.4	1.823	96.0	462.3	93.6
137	2365	531.6	.3916	.0568	2384	7822	96.0	1.877	94.8	452.6	90.2

pressure, propellant mixture ratio, fuel injection temperature, and oxidizer injection temperature. The experimentally determined wall temperatures were used and are listed in the input files in appendix A.

Boundary-layer edge conditions and wall temperatures within the combustion chamber and convergent nozzle had to be estimated because no experimental data were available. These values appear in the BLM namelist in the input files.

The TDK program requires the location of the transition from laminar to turbulent flow as input. Therefore, a study was performed to determine the approximate boundary-layer transition point within the nozzle. By comparing the experimental heat flux data to predicted heat flux, we determined that the boundary layer was laminar over the entire nozzle (ref. 8). To model the laminar flow, we instructed the program to place the transition point beyond the exit plane of the nozzle. For comparison, cases were also run for a boundary layer that transitioned to turbulent within the combustion chamber.

Appendix A contains the TDK input files for experimental readings 112 to 115, 120, 121, and 137. Only these experimental readings could be modeled because the TDK program could not run to completion for mixture ratios below 3.84. This version of the TDK program was originally written for much lower area ratio rocket nozzle conditions. The program was unable to run below an O/F of 3.84 because of the low-pressure/low-temperature conditions that are predicted as the flow expands to an area ratio of 1030.

The program was instructed to calculate the boundary-layer displacement thickness for the actual nozzle contour and to use it to obtain the displaced or inviscid contour. This inviscid contour was then run through the MOC module to obtain the final predictions of $I_{sp,V}$ and thrust.

Discussion of Results

This section presents the analytical and experimental results for an optimally contoured nozzle which expanded to an area ratio of 1030 and truncated to an exit area ratio of 427.5. The analytical results predicted by the December 1984 version of TDK for the experimental readings 112 to 115, 120, 121, and 137 are presented in table III. The corresponding experimental results are presented in table II.

By evaluating the measured heat flux from the nozzle and the estimated flow conditions within the nozzle, we determined that the boundary layer behaved as a laminar boundary layer throughout the entire nozzle (ref. 8). Thus, the TDK program was instructed to assume laminar flow in determining viscous effects. To learn the effect on predicted performance, we also made separate runs of TDK for a boundary layer that transitioned to turbulent within the combustion chamber.

In order to predict the delivered $I_{sp,V}$, TDK predictions must be adjusted to account for energy-release losses. Energy-release losses consist of two parts: vaporization losses and mixture ratio distribution losses. Vaporization losses are due

TABLE III.—TDK RESULTS

Reading	Nozzle exit expansion area ratio, ϵ	Effective chamber pressure, $P_{c,e}$		Measured propellant mixture ratio, O/F	Predicted propellant flow rate	
		kN/m ²	psia		kg/sec	lb/sec
112	1030	2482	360.0	3.84	0.5034	1.1099
113		2461	356.9	4.36	.5065	1.11667
114		2488	360.9	5.08	.5245	1.15628
115		2450	355.3	5.49	.5243	1.15595
120		2449	355.2	4.30	.5027	1.10834
121		2482	360.0	4.11	.5066	1.1169
137	427.5	2457	356.8	4.29	.5051	1.11352

Reading	Computer code					
	TDK/BLM, laminar					
	Predicted characteristic exhaust velocity, C^*		Predicted vacuum thrust, F_V		Predicted vacuum thrust coefficient, $C_{F,V}$	Predicted thrust efficiency, $\eta_{C,F,V}$ percent
	m/sec	ft/sec	N	lb		
112	2502.37	8209.89	2383.18	535.76	1.8917	96.09
113	2466.65	8092.70	2393.78	538.144	1.916	95.37
114	2408.94	7903.35	2467.18	554.644	1.9527	94.56
115	2373.03	7785.52	2452.14	551.263	1.9708	93.98
120	2473.29	8114.47	2378.05	534.607	1.9125	95.42
121	2487.25	8160.27	2399.67	539.468	1.9044	95.75
137	2473.41	8114.85	2332.30	524.321	1.8669	94.23

Reading	Computer code					
	ODE	ODK	MOC	TDK/BLM, laminar		
	Predicted vacuum specific impulse, $I_{sp,V}$ sec			Predicted vacuum specific impulse (adjusted), $I_{sp,V}$ sec	Predicted vacuum specific impulse efficiency (adjusted), $\eta_{I_{sp,V}}$ percent	
112	504.8	498.45	494.211	482.714	465.34	92.18
113	507.4	498.44	494.622	481.921	461.68	90.99
114	509.2	496.89	493.59	479.678	457.13	89.77
115	509.5	494.77	491.734	476.894	452.57	88.83
120	507.8	499.02	495.126	482.347	462.57	91.09
121	507.0	499.21	495.287	483.006	464.65	91.65
137	502.0	494.19	480.215	470.87	452.035	90.05

to incomplete liquid droplet vaporization at the nozzle throat. Mixture ratio distribution losses are due to nonuniform distribution of the vaporized propellant at the nozzle throat. As described in reference 9, experimental characteristic exhaust velocity efficiency η_{C^*} can be used as an estimate of specific impulse energy release losses. Thus, the TDK predictions were multiplied by the experimental characteristic velocity efficiencies shown in table II to account for energy-release losses. These results are labeled "Adjusted TDK/BLM" on figures 4, 5, and 8.

Performance Results—1030:1 Area Ratio Nozzle

The basic measure of rocket engine performance is specific impulse I_{sp} . In figure 4, the predicted thrust chamber losses from ideal or maximum performance are presented. The ODE curve represents the predicted ideal, one-dimensional equilibrium values of $I_{sp,V}$. The ODK curve indicates the

predicted results for one-dimensional, nonequilibrium flow. Thus, the drop in $I_{sp,V}$ from ODE to ODK represents the loss in performance due to kinetics. For the 1030:1 nozzle, these losses are estimated to be 1.3 to 2.89 percent of maximum $I_{sp,V}$ over the mixture ratio range from 3.84 to 5.49.

Points on the MOC curve are obtained from the MOC module and represent the inviscid, two-dimensional, nonequilibrium predictions. The difference between the ODK and MOC curves is the loss in performance due to nozzle divergence shape and exit angle. (The actual nozzle contour was used in these MOC calculations.) The estimated divergence losses range from 0.60 to 0.84 percent.

The TDK/BLM curve was obtained using the final results from the TDK program. These results contain the predicted boundary-layer losses from the BLM and MOC calculations for the displaced, or inviscid, contour. The difference between the MOC curve and the TDK/BLM curve is the performance loss due to laminar boundary-layer effects and is estimated to be 2.3 to 2.9 percent maximum $I_{sp,V}$ for the specified mixture ratio range.

As mentioned previously, the TDK values of $I_{sp,V}$ were adjusted to account for energy release losses. These values are shown on the adjusted TDK/BLM curves. From a point-to-point comparison, the adjusted TDK predictions for a completely laminar boundary layer are within 0.3 to 1.9 percent of the experimental readings modeled. Based on the results shown in figure 4, there appears to be no correlation between the accuracy of the prediction and the mixture ratio at which the prediction is made. The adjusted predictions for a turbulent boundary layer are 2.3 to 5.0 percent lower than the experimental results. Overall, the turbulent predictions are approximately 2.5 percent lower than the laminar predictions. This amounts to roughly a 15-sec drop in $I_{sp,V}$. Thus, proper determination of the boundary-layer characteristics prior to making a performance prediction can be important.

Figure 5 is a plot of the thrust chamber performance efficiency. Efficiency is calculated by dividing the experimental and TDK results by the ideal (ODE) values. As shown, the performance efficiency increases as mixture ratio decreases. The experimental and predicted values of efficiency compare to the same degree as in figure 4.

The vacuum thrust coefficient $C_{F,V}$ is a quantity that reflects the design quality of a nozzle. It is an indication of the thrust augmented by the gas expansion through the nozzle as compared with the thrust that would be generated if the chamber pressure acted over the throat area only. In figure 6, the experimentally obtained values of $C_{F,V}$ are presented along with the TDK predictions for a completely laminar boundary layer and the TDK predictions for a turbulent boundary layer. As indicated in the plot, thrust produced by the nozzle increased as mixture ratio increased. The difference between the experimental and TDK/BLM laminar results is within ± 1.3 percent. For a turbulent boundary layer, the predictions fall approximately 3.5 percent below the experimental results.

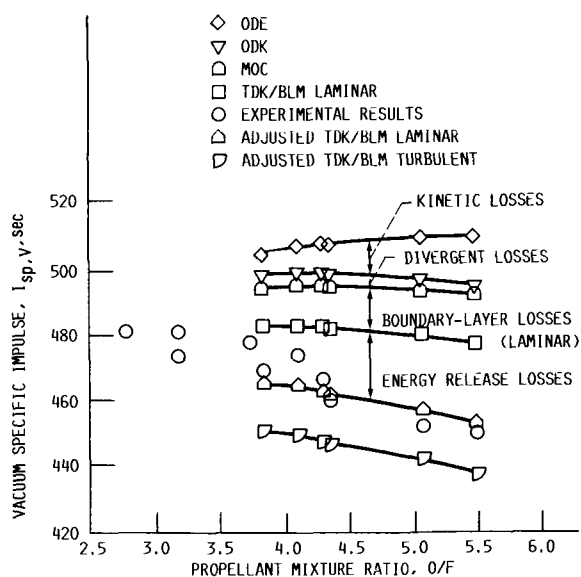


Figure 4.—Predicted thrust chamber losses from ideal performance. Area ratio, ϵ , 1030.

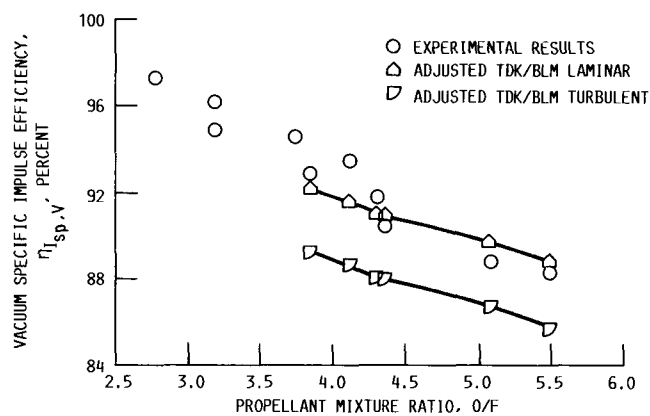


Figure 5.—Thrust chamber performance efficiency. Area ratio, ϵ , 1030. Specific impulse efficiency $\eta_{I_{sp}}$ is based on ideal one-dimensional equilibrium (ODE) results.

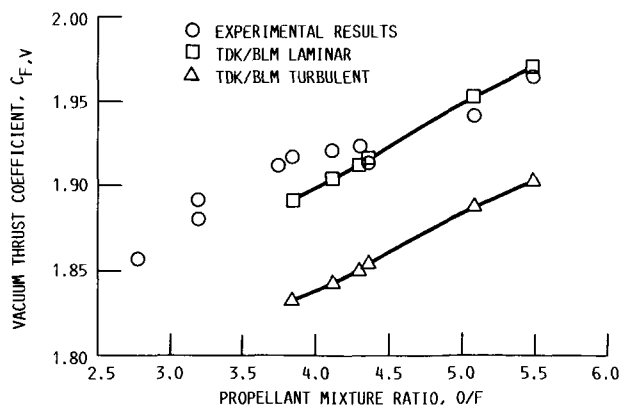


Figure 6.—Experimental and predicted vacuum thrust coefficient. Area ratio, ϵ , 1030.

Figure 7 is a plot of the vacuum thrust coefficient efficiency based on ideal results for the 1030:1 nozzle. As shown previously with performance efficiency, vacuum thrust efficiency increases as the mixture ratio decreases. These curves compare in the same manner as those in figure 6.

Performance Results—Truncated Contour

The TDK program was used to model the experimental results for the truncated contour and the test conditions in reading 137. For $I_{sp,V}$ the program predicted 1.6-percent kinetic losses, 2.8-percent divergence losses, and 1.9-percent laminar boundary-layer losses. After adjusting the TDK/BLM laminar $I_{sp,V}$ prediction for energy release losses, the prediction of 452.04 sec was within 0.12 percent of the experimental value of 452.6 sec. A turbulent boundary-layer assumption for this configuration yields an $I_{sp,V}$ of 441.28 sec (2.5 percent lower than the experimental $I_{sp,V}$).

The predicted $C_{F,V}$ for the truncated contour with a completely laminar boundary layer is 1.8669 and is within 0.5 percent of the experimental value of 1.877. The TDK prediction for the truncated contour with a turbulent boundary layer yields a $C_{F,V}$ that is 2.9 percent lower than the experimental $C_{F,V}$.

The nozzle was truncated to experimentally determine the performance gain between the area ratios of 427.5 and 1030 and to validate predictions of performance over the length of the nozzle. Figure 8 is a plot of the predicted $I_{sp,V}$ over the length of the 1030:1 nozzle for a mixture ratio of 4.3. The two points plotted indicate the experimental values of $I_{sp,V}$ obtained from the full and truncated contours. As shown, there is very good agreement between the TDK laminar predictions and the experimental results. The TDK turbulent predictions fall approximately 10 to 20 sec below the laminar curve between an area ratio of 100 and the exit.

Pressure Integration Results

Figure 9 is a plot of the wall static pressure distribution for the 1030:1 nozzle. It is expressed as the ratio of wall static pressure P_w to effective chamber pressure $P_{c,e}$ for reading 115. Effective chamber pressure is an estimate of nozzle throat total pressure. The method used to obtain $P_{c,e}$ is discussed in reference 3. There are two significant observations to be drawn from this figure. The first observation indicates whether the nozzle is flowing full or whether the flow has separated from the wall. For the experimental data reported, there was no separation, as the pressure distribution continued to expand all the way to the exit plane of the nozzle. The second observation compares experimental and analytically predicted values of pressure. TDK predicted static pressures are within ± 5 percent over most of the nozzle. The greatest difference between prediction and experiment is at the area ratios of 12 and 1000. At these points, the experimental values are approximately 15 percent higher. This could be an indication

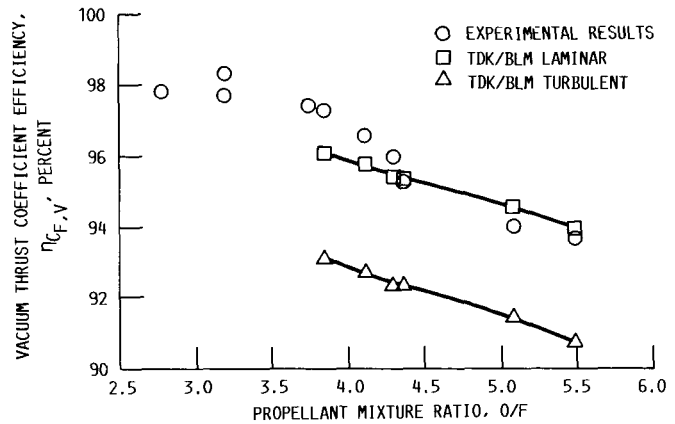


Figure 7.—Efficiency of thrust amplification based on one-dimensional equilibrium (ODE) results. Area ratio, ϵ , 1030.

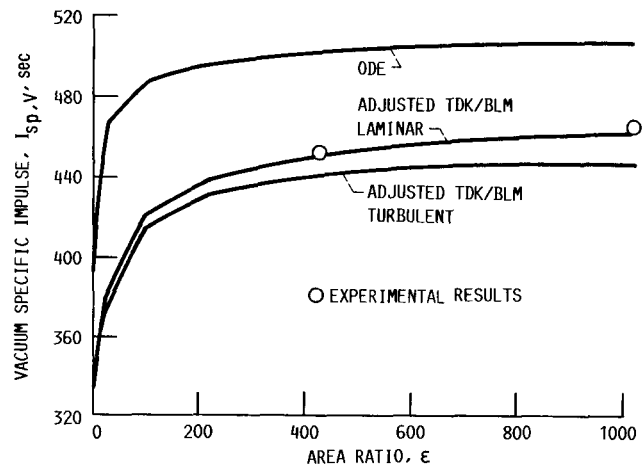


Figure 8.—Predicted and experimental thrust chamber performance over length of nozzle. Area ratio, ϵ , 1030.

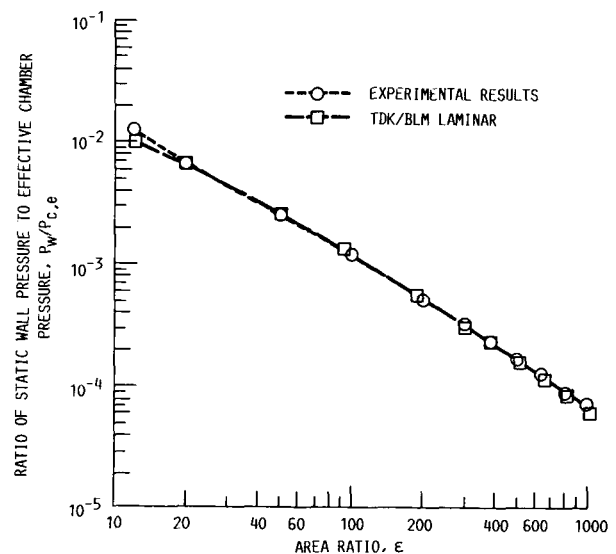


Figure 9.—Static wall pressure distribution for extended nozzle. Reading 115; area ratio, ϵ , 1030; propellant mixture ratio, O/F , 5.49; effective chamber pressure, $P_{c,e}$, 2450 kN/m² (355.3 psia).

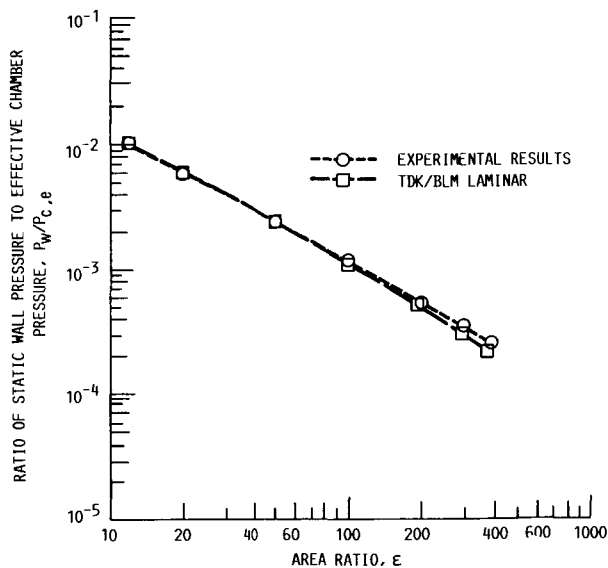


Figure 10.—Static wall pressure distribution for truncated nozzle. Reading 137; area ratio, ϵ , 427.5; propellant mixture ratio, O/F , 4.29; effective chamber pressure, $P_{c,e}$, 2460 kN/m² (356.8 psia).

of separated flow near the throat and of boundary-layer feedback at the exit. Both of these phenomena would result in a higher pressure measurement than predicted. Further investigation into this matter is beyond the scope of this report.

Figure 10 is the wall static pressure distribution for the truncated nozzle (reading 137). The TDK predicted pressures are within ± 5 percent of experimental pressures, except for area ratios of approximately 300 to the exit. Over this part of the nozzle, the experimental values are approximately 15 percent higher than predicted values. Because the result of this comparison was not the same as that for the full contour, a comparison was made of the pressures measured in readings 113 (full contour) and 137 (truncated contour). In both cases, $P_{c,e}$ and O/F were similar. The comparison indicated that the pressures measured at the same area ratios agreed to within ± 0.5 percent up to an area ratio of 200. For the pressures measured at area ratios of 200, 300, and 388, the values were 5 to 10 percent higher for reading 137. This indicates that truncating the nozzle affected the experimental static pressure measurements, which may explain the 15-percent difference between experimental and theoretical values in figure 10. The higher pressures could be occurring as a result of the response of the subsonic boundary layer to the change in capsule pressure from reading 113 to reading 137. Further testing is needed to study this phenomenon.

A calculation was performed using the measured wall static pressure distribution for the 1030:1 nozzle. The area under the pressure plot was determined from an area ratio of 427.5 to 1030. This pressure integration yields the experimental inviscid thrust gain achieved with the addition of the nozzle extension from 427.5:1 to 1030:1. When the actual thrust gain (the difference in measured thrust for the full and truncated contours) is subtracted from the inviscid thrust gain, the result

is the shear or drag force that is produced between the area ratios of 427.5 and 1030. A detailed discussion of the pressure integration procedure appears in appendix B.

Integration of the measured static pressures between the area ratios of 427.5 and 1030 yielded values of 80.07 N (18.0 lb), or 3.35 percent of the total vacuum thrust, at a mixture ratio of 3.04 and 82.69 N (18.59 lb), or 3.40 percent of the total vacuum thrust, at a mixture ratio of 4.29. The measured thrust gain at those mixture ratios was 69.21 N (15.56 lb), or 2.90 percent, and 55.69 N (12.52 lb), or 2.29 percent, respectively. Thus, the shear or drag force was as follows:

	Mixture ratio	
	3.04	4.29
Inviscid thrust gain, N (lb)	80.07 (18.00)	82.69 (18.59)
Actual thrust gain, N (lb)	69.21 (15.56)	55.69 (12.52)
Drag, N (lb)	^a 10.86 (2.44)	^a 27.00 (6.07)
Vacuum thrust, percent of total	0.45	1.11

^aActual thrust gain subtracted from inviscid thrust gain.

The corresponding TDK predictions at a mixture ratio of 4.29 were 62.34 N (14.015 lb) inviscid thrust, or 2.67 percent of the total vacuum thrust, and 45.75 N (10.286 lb), or 1.96 percent of the thrust gain. Therefore, the predicted shear or drag force was as follows:

Mixture ratio	4.29
Inviscid thrust gain, N (lb)	62.34 (14.02)
Actual thrust gain, N (lb)	45.75 (10.29)
Drag, N (lb)	^a 16.59 (3.73)
Vacuum thrust, percent of total	0.71

^aActual thrust gain subtracted from inviscid thrust gain.

Thus, the TDK prediction of drag was lower than the experimental value by 10.23 N (2.3 lb), or 0.4 percent of the total vacuum thrust.

Figure 11 was developed by extending the examination of inviscid thrust and drag decrement. In this figure, the predicted

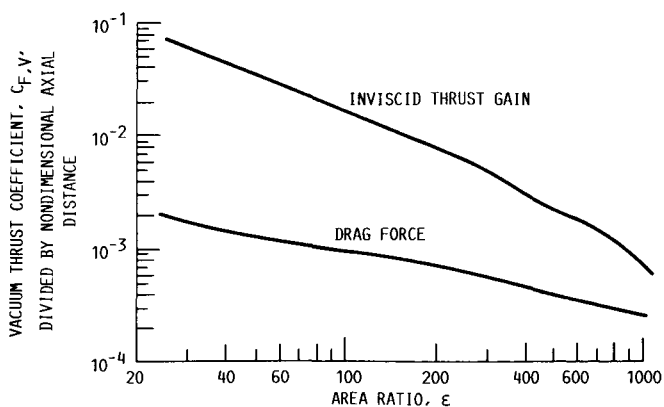


Figure 11.—Predicted thrust gain over length of nozzle. Reading 115; area ratio, ϵ , 1030; propellant mixture ratio, O/F , 5.49. Nondimensional axial distance is axial distance divided by throat radius.

drag force and predicted inviscid thrust produced per unit length of axial distance are plotted for the 1030:1 nozzle at a mixture ratio of 5.49 (reading 115). The distance between the curves represent the actual thrust gain per unit length for a specific area ratio. An analysis of this kind could be used to examine the advantage of either extending a nozzle contour or truncating it. As the need for higher area ratio nozzles develops, the examination of thrust gain with area ratio will become more important.

Summary of Results

Predictions from the December 1984 version of the TDK nozzle analysis program were compared to experimental results of a test-fired rocket nozzle. The hardware tested was a heat-sink nozzle optimally expanded to an area ratio of 1030 and designed so that it could be truncated at an area ratio of 427.5. Test conditions, which included mixture ratio, propellant (gaseous oxygen and gaseous hydrogen) temperatures, chamber pressure, and nozzle wall temperatures, were used in the computer program to accurately model the nozzle performance.

An evaluation of the measured heat flux from the nozzle and the estimated flow conditions within the nozzle determined that the boundary layer behaved as a laminar boundary layer throughout the entire nozzle. Thus, the TDK program was instructed to assume laminar flow in determining viscous effects. To learn the effect on predicted performance, we also made separate runs of TDK for a boundary layer that transitioned to turbulent within the combustion chamber. The TDK predictions indicated that a 2.5-percent difference in vacuum specific impulse can result from using a turbulent boundary-layer assumption, instead of a completely laminar boundary-layer assumption. Thus, proper determination of the boundary-layer characteristics prior to making a performance prediction can be important.

The TDK predictions were compared to the experimental results for the full and truncated contours. The parameters that were compared were vacuum specific impulse, vacuum specific impulse efficiency, vacuum thrust coefficient, vacuum thrust coefficient efficiency, wall static pressure, and thrust gain between the area ratios of 427.5 and 1030. The results of the comparison for the mixture ratio range from 3.84 to 5.49 were as follows:

1. The TDK predictions of delivered vacuum specific impulse were within 0.12 to 1.9 percent of the experimental results. There appears to be no correlation between the accuracy of the prediction and the mixture ratio at which the prediction was made. The experimental and predicted values of efficiency compare to the same degree.

2. Vacuum thrust coefficient predictions were within ± 1.3 percent of experimental results. Again, the predictions of thrust coefficient efficiency compare to the same degree.

3. The predictions of wall static pressure were within ± 5 percent of experimental results, except at the lowest and highest area ratios at which they were measured. At these area ratios of 12 and ~ 1000 , the predictions were 15 percent lower than measured results.

4. An experimental value for inviscid thrust was obtained for the nozzle extension between area ratios of 427.5 and 1030 by using an integration of the measured wall static pressures. Subtracting the measured thrust gain produced by the nozzle between area ratios of 427.5 and 1030 from the inviscid thrust gain yielded experimental drag decrements of 10.86 and 27.00 N (2.44 and 6.07 lb) for mixture ratios of 3.04 and 4.29, respectively. These values correspond to 0.45 and 1.11 percent of the total vacuum thrust. At a mixture ratio of 4.29, the TDK predicted drag decrement was 16.59 N (3.73 lb), or 0.71 percent total vacuum thrust.

Lewis Research Center
National Aeronautics and Space Administration
Cleveland, Ohio, May 6, 1987

Appendix A TDK Input Files

Input for Reading 112

LOW T CPHS			
H		2	
100.	4.968		1
200.	4.968		2
H2		2	
100.	6.729		1
200.	6.560		2
H2O		2	
100.	7.961		1
200.	7.969		2
O		2	
100.	5.665		1

200. 5.433 2 2
 OH 2
 100. 7.798 1
 200. 7.356 2
 O2 2
 100. 6.956 1
 200. 6.961 2

END LOW T CPHS

TITLE HIGH E NOZZLE STUDY: E=1000 AND READING = 112

DATA

EDATA

ODE=1,ODK=1,TDK=1,BLM=1,IRPEAT=2,IOFF=6,
 RSI=0.5,ASUB=3.,1.5,NASUB=2,IRSTRT=0,
 ASUP=1.5,2.0,30.0,200.0,400.0,600.0,1024.0,NASUP=7,
 ECRAT=4.223,RI=2.,THETA=25.,RWTU=2.,
 ITYPE=0,IWALL=4,RWTD=0.4,THETA=39.41,
 THE=7.94,NWS=36,

RS= 0.0000, 1.1316, 1.1780, 1.2748,
 1.3704, 1.4198, 1.7658, 2.0876,
 2.4916, 3.0372, 5.2522, 5.7028,
 6.5606, 7.0420, 7.5072, 8.0464,
 9.0636, 9.5394, 10.6852, 12.0244,
 12.7284, 14.0056, 15.2408, 15.9610,
 16.6554, 17.3210, 18.7560, 19.6768, 20.5562,
 21.6918, 23.7554, 24.6744, 27.0428,
 29.1286, 30.1862, 32.0156,

ZS= 0.0000, 0.3094, 0.3654, 0.4778,
 0.5908, 0.6480, 1.0430, 1.4050,
 1.8722, 2.5246, 5.5320, 6.2150,
 7.5802, 8.3862, 9.1920, 10.1592,
 12.0810, 13.0230, 15.4056, 18.4006,
 20.0684, 23.2606, 26.5588, 28.5824,
 30.6060, 32.6136, 37.1806, 40.2916, 43.4026,
 47.6334, 55.9914, 60.0166, 71.3698,
 82.7063, 89.0425, 101.2383,

END

REACTANTS

H 2.	00	100.	G285.60	F
O 2.	00	100.	G279.20	O

NAMELISTS

EDATA

RKT=T,P=360.0,PSIA=T,OF=T,OFSKED=3.84,
 SUPAR=30.0,200.0,400.0,600.0,1024.0,ECRAT=4.223,

END

REACTIONS

H + OH = H2O , A=8.4E21 , N=2.0 , B=0., (AR) BAULCH 72 (A) 10U
 O + H = OH , A=3.62E18 , N=1. , B=0., (AR) JENSEN 78 (B) 30U
 O + O = O2 , A=1.9E13 , N=0. , B=-1.79, (AR) BAULCH 76 (A) 10U
 H + H = H2 , A=6.4E17 , N=1. , B=0., (AR) BAULCH 72 (A) 30U

END TBR REAX

H2 + OH = H2O + H , A=2.20E13, N=0.00, B=5.15, BAULCH 72 (A) 2U
 OH + OH = H2O + O , A=6.30E12, N=0.00, B=1.09, BAULCH 72 (A) 3U
 H2 + O = H + OH , A=1.80E10, N=-1. , B=8.9, BAULCH 72 (A) 1.5U
 O2 + H = O + OH , A=2.2E14 , N=0. , B=16.8, BAULCH 72 (A) 1.5U

LAST REAX

THIRD BODY REAX RATE RATIOS

SPECIES H2,5.,5.,5.,4.,
 SPECIFS H2O,17.,5.,5.,10.,
 SPECIES O2,6.,5.,11.,1.5,
 SPECIES H,12.5,12.5,12.5,25.,
 SPECIES O,12.5,12.5,12.5,25.,
 SPECIES OH,12.5,12.5,12.5,25.,

LAST CARD

EDOK

EP=0.0,JPRNT=-2,MAVISP=1,XM(1)=1.0,NJPRNT=7,
 HI=0.01,HMIN=0.01,HMAX=0.01,

END

ETRANS

MP=200,

END

EMOC

```

EXITPL=.FALSE.,EPW=0.05,
&END
&BLM
IHFLAG=0,NTQW=19,
TQW=1260.0,1260.0,1260.0,2770.0,3330.0,3960.0,4050.0,
1008.61,1039.24,886.05,610.30,571.14,549.45,
528.76,538.35,520.14,530.12,516.42,525.62,
XTQW= -13.0,-6.0,-2.26,-2.14,-1.57,-0.89,0.0,
1.8722,3.06,4.406,8.4344,13.9624,
23.6164,32.6124,40.3644,50.2504,62.4584,77.9624,95.7704,
APROF=30.,200.,400.0,1009.0,NPROF=4,KDTPLT=1,
KMTPLT=1,KTWPLT=1,XSEG=-14.0,10.0,33.0,56.0,79.0,101.23,NSEGS=5,
XINO(1)=-14.0,-12.0,-10.0,-8.0,-6.0,-4.0,
RINO(1)=2.054,2.054,2.054,2.054,2.054,2.054,
UEO(1)=81.0,216.0,351.0,486.0,621.0,757.0,
TEO(1)=5450.0,5449.6,5448.4,5446.2,5444.0,5442.8,
PEO(1)=360.0,359.6,358.3,357.65,356.0,355.9,
NTR=700,
&END

```

Input for Reading 113

```

LOW T CPHS
H          2
100.      4.968          1
200.      4.968          2
H2         2
100.      6.729          1
200.      6.560          2
H2O        2
100.      7.961          1
200.      7.969          2
O           2
100.      5.665          1
200.      5.433          2
OH          2
100.      7.798          1
200.      7.356          2
O2         2
100.      6.956          1
200.      6.961          2
END LOW T CPHS

```

TITLE HIGH E NOZZLE STUDY: E=1000 AND READING = 113

DATA

&DATA

```

ODE=1,CDK=1,TDK=0,BLM=0,IRPEAT=0,IOFF=6,
RSI=0.5,ASUB=3.,1.5,NASUB=2,IRSTRT=0,
ASUP=1.5,2.0,30.0,200.0,400.0,600.0,1024.0,NASUP=7,
ECRAT=4.223,RI=2.,THETA=25.,RWTU=2.,
ITYPE=0,IWALL=4,RWTD=0.4,THETA=39.41,
THE=7.94,NWS=36,
RS= 0.0000, 1.1316, 1.1780, 1.2748,
1.3704, 1.4198, 1.7658, 2.0876,
2.4916, 3.0372, 5.2522, 5.7028,
6.5606, 7.0420, 7.5072, 8.0464,
9.0636, 9.5394, 10.6852, 12.0244,
12.7284, 14.0056, 15.2408, 15.9610,
16.6554, 17.3210, 18.7560, 19.6768, 20.5562,
21.6918, 23.7554, 24.6744, 27.0428,
29.1286, 30.1862, 32.0156,
ZS= 0.0000, 0.3094, 0.3654, 0.4778,
0.5908, 0.6480, 1.0430, 1.4050,
1.8722, 2.5246, 5.5320, 6.2150,
7.5802, 8.3862, 9.1920, 10.1592,
12.0810, 13.0230, 15.4056, 18.4006,
20.0684, 23.2606, 26.5588, 28.5824,
30.6060, 32.6136, 37.1806, 40.2916, 43.4026,
47.6334, 55.9914, 60.0166, 71.3698,
82.7063, 89.0425, 101.2383,
&END

```

```

REACTANTS
H 2.          00      100.      G284.20 F
O 2.          00      100.      G277.00 O

```

NAMELISTS

```

&ODE
RKT=T,P=356.9,PSIA=T,OF=T,OFSKED=4.36,
SUPAR=30.0,200.0,400.0,600.0,1024.0,ECRAT=4.223,
&END

```

REACTIONS

```

H + OH = H2O      , A=8.4E21 , N=2.0 , B=0., (AR) BAULCH 72 (A) 10U
O + H = OH        , A=3.62E18 , N=1.  , B=0., (AR) JENSEN 78 (B) 30U
O + O = O2        , A=1.9E13 , N=0.  , B=-1.79, (AR) BAULCH 76 (A) 10U
H + H = H2        , A=6.4E17 , N=1.  , B=0., (AR) BAULCH 72 (A) 30U
END TBR REAX
H2 + OH = H2O + H , A=2.20E13, N=0.00, B=5.15, BAULCH 72 (A) 2U
OH + OH = H2O + O , A=6.30E12, N=0.00, B= 1.09, BAULCH 72 (A) 3U
H2 + O = H + OH   , A=1.80E10, N=-1.  , B=8.9,  BAULCH 72 (A) 1.5U
O2 + H = O + OH   , A=2.2E14 , N=0.  , B=16.8, BAULCH 72 (A) 1.5U

```

LAST REAX

```

THIRD BODY REAX RATE RATIOS
SPECIES H2,5.,5.,5.,4.,
SPECIES H2O,17.,5.,5.,10.,
SPECIES O2,6.,5.,11.,1.5,
SPECIES H,12.5,12.5,12.5,25.,
SPECIES O,12.5,12.5,12.5,25.,
SPECIES OH,12.5,12.5,12.5,25.,

```

LAST CARD

```

&ODK
EP=10.0,JPRNT=-2,MAVISP=1,XM(1)=1.0,NJPRNT=7,
HI=0.01,HMIN=0.01,HMAX=0.01,
&END
&TRANS
MP=200,
&END
&MOC
EXITPL=.FALSE.,EPW=0.05,
&END
&BLM
IHFLAG=0,NTQW=19,
TQW=1260.0,1260.0,1260.0,1260.0,2770.0,3330.0,3960.0,4050.0,
1061.73,1080.00,934.61,641.91,600.62,574.11,
551.50,555.18,536.63,541.40,528.52,533.44,
XTQW= -13.0,-6.0,-2.26,-2.14,-1.57,-0.89,0.0,
1.8722,3.06,4.406,8.4344,13.9624,
23.6164,32.6124,40.3644,50.2504,62.4584,77.9624,95.7704,
APROF=30.,200.,400.0,1009.0,NPROF=4,KDTPLT=1, NTR=700,
KMTPLT=1,KTWPLT=1,XSEG=-14.0,10.0,33.0,56.0,79.0,101.23,NSEGS=5,
XINO(1)=-14.0,-12.0,-10.0,-8.0,-6.0,-4.0,
RINO(1)=2.054,2.054,2.054,2.054,2.054,2.054,
UEO(1)=80.0,213.0,346.0,480.0,613.0,746.0,
TEO(1)=5731.8,5731.0,5729.7,5728.2,5726.0,5724.8,
PEO(1)=356.9,356.0,355.3,354.65,353.0,352.9,
&END

```

Input for Reading 114

LOW T CPHS

```

H          2
100.      4.968          1
200.      4.968          2
H2         2
100.      6.729          1
200.      6.560          2
H2O        2
100.      7.961          1
200.      7.969          2
O           2
100.      5.665          1
200.      5.433          2

```

```

OH                2
100.             7.798
200.             7.356
O2               2
100.             6.956
200.             6.961
END LOW T CPHS

```

```

TITLE HIGH E NOZZLE STUDY: E=1000 AND READING = 114
DATA

```

```

&DATA
ODE=1,ODK=1,TDK=1,BLM=1,IRPEAT=2,IOFF=6,
RSI=0.5,ASUB=3.,1.5,NASUB=2,IRSTRT=0,
ASUP=1.5,2.0,30.0,200.0,400.0,600.0,1024.0,NASUP=7,
ECRAT=4.223,RI=2.,THETA=25.,RWTU=2.,
ITYPE=0,IWALL=4,RWTD=0.4,THETA=39.41,
THE=7.94,NWS=36,
RS= 0.0000, 1.1316, 1.1780, 1.2748,
    1.3704, 1.4198, 1.7658, 2.0876,
    2.4916, 3.0372, 5.2522, 5.7028,
    6.5606, 7.0420, 7.5072, 8.0464,
    9.0636, 9.5394, 10.6852, 12.0244,
    12.7284, 14.0056, 15.2408, 15.9610,
    16.6554, 17.3210, 18.7560, 19.6768, 20.5562,
    21.6918, 23.7554, 24.6744, 27.0428,
    29.1286, 30.1862, 32.0156,
ZS= 0.0000, 0.3094, 0.3654, 0.4778,
    0.5908, 0.6480, 1.0430, 1.4050,
    1.8722, 2.5246, 5.5320, 6.2150,
    7.5802, 8.3862, 9.1920, 10.1592,
    12.0810, 13.0230, 15.4056, 18.4006,
    20.0684, 23.2606, 26.5588, 28.5824,
    30.6060, 32.6136, 37.1806, 40.2916, 43.4026,
    47.6334, 55.9914, 60.0166, 71.3698,
    82.7063, 89.0425, 101.2383,

```

```

&END
REACTANTS
H 2.             00          100.      0.0      G283.90 F
O 2.             00          100.      0.0      G275.80 O

```

```

NAMELISTS
&CODE
RKT=T,P=360.9,PSIA=T,OF=T,OFSKED=5.08,
SUPAR=30.0,200.0,400.0,600.0,1024.0,ECRAT=4.223,
&END

```

```

REACTIONS
H + OH = H2O      , A=8.4E21 , N=2.0 , B=0., (AR) BAULCH 72 (A) 10U
O + H = OH        , A=3.62E18 , N=1. , B=0., (AR) JENSEN 78 (B) 30U
O + O = O2        , A=1.9E13 , N=0. , B=-1.79, (AR) BAULCH 76 (A) 10U
H + H = H2        , A=6.4E17 , N=1. , B=0., (AR) BAULCH 72 (A) 30U
END TBR REAX
H2 + OH = H2O + H , A=2.20E13, N=0.00, B=5.15, BAULCH 72 (A) 2U
OH + OH = H2O + O , A=6.30E12, N=0.00, B= 1.09, BAULCH 72 (A) 3U
H2 + O = H + OH   , A=1.80E10, N=-1. , B=8.9, BAULCH 72 (A) 1.5U
O2 + H = O + OH   , A=2.2E14 , N=0. , B=16.8, BAULCH 72 (A) 1.5U

```

```

LAST REAX
THIRD BODY REAX RATE RATIOS
SPECIES H2,5.,5.,5.,4.,
SPECIES H2O,17.,5.,5.,10.,
SPECIES O2,6.,5.,11.,1.5,
SPECIES H,12.5,12.5,12.5,25.,
SPECIES O,12.5,12.5,12.5,25.,
SPECIES OH,12.5,12.5,12.5,25.,

```

```

LAST CARD
&ODK
EP=0.0,JPRNT=-2,MAVISP=1,XM(1)=1.0,NJPRNT=7,
HI=0.01,HMIN=0.01,HMAX=0.01,
&END
&TRANS
MP=200,
&END
&MOC
EXITPL=.FALSE.,EPW=0.05,
&END

```

EBLM

IHFLAG=0,NTQW=17,
 TQW=1260.0,2770.0,3330.0,3960.0,4050.0,
 1169.58,1128.31,972.62,663.76,618.64,589.39,
 567.31,569.98,548.78,549.66,535.97,537.46,
 XTQW= -2.26,-2.14,-1.57,-0.89,0.0,
 1.8722,3.06,4.406,8.4344,13.9624,
 23.6164,32.6124,40.3644,50.2504,62.4584,77.9624,95.7704,
 APROF=30.,200.,400.0,1009.0,NPROF=4,KDTPLT=1,
 KMTPLT=1,KTWPLT=1,XSEG=-14.0,10.0,33.0,56.0,79.0,101.23,NSEGS=5,
 XINO(1)=-14.0,-12.0,-10.0,-8.0,-6.0,-4.0,
 RINO(1)=2.054,2.054,2.054,2.054,2.054,2.054,
 UEO(1)=35.0,165.0,300.0,425.0,560.0,685.0,
 TEO(1)=6014.8,6013.6,6012.4,6011.2,6010.0,6008.8,
 PEO(1)=360.7,360.0,359.3,358.65,358.0,357.3,
 NTR=800,
 EEND

Input for Reading 115

LOW T CPHS

H		2		
100.	4.968			1
200.	4.968			2
H2		2		
100.	6.729			1
200.	6.560			2
H2O		2		
100.	7.961			1
200.	7.969			2
O		2		
100.	5.665			1
200.	5.433			2
OH		2		
100.	7.798			1
200.	7.356			2
O2		2		
100.	6.956			1
200.	6.961			2

END LOW T CPHS

TITLE HIGH E NOZZLE STUDY: E=1000 AND READING = 115

DATA

EADATA

ODE=1,ODK=1,TDK=1,BLM=1,IRPEAT=2,IOFF=6,
 RSI=0.5,ASUB=3.,1.5,NASUB=2,IRSTR=2,
 ASUP=1.5,2.0,30.0,200.0,400.0,600.0,1024.0,NASUP=7,
 ECRAT=4.223,RI=2.,THETA=25.,RWTU=2.,
 ITYPE=0,IWALL=4,RWTD=0.4,THETA=39.41,
 THE=7.94,NWS=36,

RS= 0.0000, 1.1316, 1.1780, 1.2748,
 1.3704, 1.4198, 1.7658, 2.0876,
 2.4916, 3.0372, 5.2522, 5.7028,
 6.5606, 7.0420, 7.5072, 8.0464,
 9.0636, 9.5394, 10.6852, 12.0244,
 12.7284, 14.0056, 15.2408, 15.9610,
 16.6554, 17.3210, 18.7560, 19.6768, 20.5562,
 21.6918, 23.7554, 24.6744, 27.0428,
 29.1286, 30.1862, 32.0156,
 ZS= 0.0000, 0.3094, 0.3654, 0.4778,
 0.5908, 0.6480, 1.0430, 1.4050,
 1.8722, 2.5246, 5.5320, 6.2150,
 7.5802, 8.3862, 9.1920, 10.1592,
 12.0810, 13.0230, 15.4056, 18.4006,
 20.0684, 23.2606, 26.5588, 28.5824,
 30.6060, 32.6136, 37.1806, 40.2916, 43.4026,
 47.6334, 55.9914, 60.0166, 71.3698,
 82.7063, 89.0425, 101.2383,

EEND

REACTANTS

H 2.	00	100.	G283.50	F
O 2.	00	100.	G275.90	O

NAMELISTS

CODE

RKT=T,P=355.3,PSIA=T,OF=T,OFSKED=5.49,
 SUPAR=30.0,200.0,400.0,600.0,1024.0,ECRAT=4.223,

END

REACTIONS

H + OH = H2O , A=8.4E21 , N=2.0 , B=0. , (AR) BAULCH 72 (A) 10U
 O + H = OH , A=3.62E18 , N=1. , B=0. , (AR) JENSEN 78 (B) 30U
 O + O = O2 , A=1.9E13 , N=0. , B=-1.79 , (AR) BAULCH 76 (A) 10U
 H + H = H2 , A=6.4E17 , N=1. , B=0. , (AR) BAULCH 72 (A) 30U

END TBR REAX

H2 + OH = H2O + H , A=2.20E13 , N=0.00 , B=5.15 , BAULCH 72 (A) 2U
 OH + OH = H2O + O , A=6.30E12 , N=0.00 , B= 1.09 , BAULCH 72 (A) 3U
 H2 + O = H + OH , A=1.80E10 , N=-1. , B=8.9 , BAULCH 72 (A) 1.5U
 O2 + H = O + OH , A=2.2E14 , N=0. , B=16.8 , BAULCH 72 (A) 1.5U

LAST REAX

THIRD BODY REAX RATE RATIOS

SPECIES H2,5.,5.,5.,4.,
 SPECIES H2O,17.,5.,5.,10.,
 SPECIES O2,6.,5.,11.,1.5,
 SPECIES H,12.5,12.5,12.5,25.,
 SPECIES O,12.5,12.5,12.5,25.,
 SPECIES OH,12.5,12.5,12.5,25.,

LAST CARD

END

EP=0.0,JPRNT=-2,MAVISP=1,XM(1)=1.0,NJPRNT=7,
 HI=0.01,HMIN=0.01,HMAX=0.01,

END

STRANS

MP=200,

END

EMOC

EXITPL=.FALSE.,EPW=0.05,

END

EBLM

IHFLAG=0,NTQW=19,
 TQW=1260.0,1260.0,1260.0,2770.0,3330.0,3960.0,4050.0,
 1156.32,1117.60,985.76,682.10,637.87,603.26,
 581.66,579.76,559.11,557.71,542.84,542.02,
 XTQW= -13.0,-6.0,-2.26,-2.14,-1.57,-0.89,0.0,
 1.8722,3.06,4.406,8.4344,13.9624,
 23.6164,32.6124,40.3644,50.2504,62.4584,77.9624,95.7704,
 APROF=30.,200.,400.0,1009.0,NPROF=4,KDTPLT=1, NTR=800,
 KMTPLT=1,KTWPLT=1,XSEG=-14.0,10.0,33.0,56.0,79.0,101.23,NSEGS=5,
 XINO(1)=-14.0,-12.0,-10.0,-8.0,-6.0,-4.0,
 RIMO(1)=2.054,2.054,2.054,2.054,2.054,2.054,
 UEO(1)=80.0,213.0,346.0,480.0,613.0,746.0,
 TEO(1)=6124.7,6123.8,6122.0,6120.2,6119.0,6118.0,
 PEO(1)=355.3,355.0,354.3,353.65,352.9,352.0,

END

Input for Reading 120

LOW T CPHS

H		2	
100.	4.968		1
200.	4.968		2
H2		2	
100.	6.729		1
200.	6.560		2
H2O		2	
100.	7.961		1
200.	7.969		2
O		2	
100.	5.665		1
200.	5.433		2
OH		2	
100.	7.798		1
200.	7.356		2
O2		2	

100. 6.956 1
200. 6.961 2
END LOW T CPHS
TITLE HIGH E NOZZLE STUDY: E=1000 AND READING = 120
DATA

CDATA

ODE=1,ODK=1,TDK=0,BLM=0,IRPEAT=0,IOFF=6,
RSI=0.5,ASUB=3.,1.5,NASUB=2,IPSTRT=0,
ASUP=1.5,2.0,30.0,200.0,400.0,600.0,1024.0,NASUP=7,
ECRAT=4.223,RI=2.,THETA=25.,RWTU=2.,
ITYPE=0,IWALL=4,RWTD=0.4,THETA=39.41,
THE=7.94,NWS=36,

RS= 0.0000, 1.1316, 1.1780, 1.2748,
1.3704, 1.4198, 1.7658, 2.0876,
2.4916, 3.0372, 5.2522, 5.7028,
6.5606, 7.0420, 7.5072, 8.0464,
9.0636, 9.5394, 10.6852, 12.0244,
12.7284, 14.0056, 15.2408, 15.9610,
16.6554, 17.3210, 18.7560, 19.6768, 20.5562,
21.6918, 23.7554, 24.6744, 27.0428,
29.1286, 30.1862, 32.0156,
ZS= 0.0000, 0.3094, 0.3654, 0.4778,
0.5908, 0.6480, 1.0430, 1.4050,
1.8722, 2.5246, 5.5320, 6.2150,
7.5802, 8.3862, 9.1920, 10.1592,
12.0810, 13.0230, 15.4056, 18.4006,
20.0684, 23.2606, 26.5588, 28.5824,
30.6060, 32.6136, 37.1806, 40.2916, 43.4026,
47.6334, 55.9914, 60.0166, 71.3698,
82.7063, 89.0425, 101.2383,

END

REACTANTS

H 2.	00	100.	G294.40	F
O 2.	00	100.	G287.50	O

NAMELISTS

CODE

RKT=T,P=355.2,PSIA=T,OF=T,OFSKED=4.30,
SUPAR=30.0,200.0,400.0,600.0,1024.0,ECRAT=4.223,

END

REACTIONS

H + OH = H2O , A=8.4E21 , N=2.0 , B=0., (AR) BAULCH 72 (A) 10U
O + H = OH , A=3.62E18 , N=1. , B=0., (AR) JENSEN 78 (B) 30U
O + O = O2 , A=1.9E13 , N=0. , B=-1.79, (AR) BAULCH 76 (A) 10U
H + H = H2 , A=6.4E17 , N=1. , B=0., (AR) BAULCH 72 (A) 30U

END TBR REAX

H2 + OH = H2O + H , A=2.20E13, N=0.00, B=5.15, BAULCH 72 (A) 2U
OH + OH = H2O + O , A=6.30E12, N=0.00, B= 1.09, BAULCH 72 (A) 3U
H2 + O = H + OH , A=1.80E10, N=-1. , B=8.9, BAULCH 72 (A) 1.5U
O2 + H = O + OH , A=2.2E14 , N=0. , B=16.8, BAULCH 72 (A) 1.5U

LAST REAX

THIRD BODY REAX RATE RATIOS

SPECIES H2,5.,5.,5.,4.,
SPECIES H2O,17.,5.,5.,10.,
SPECIES O2,6.,5.,11.,1.5,
SPECIES H,12.5,12.5,12.5,25.,
SPECIES O,12.5,12.5,12.5,25.,
SPECIES OH,12.5,12.5,12.5,25.,

LAST CARD

END

EP=10.0,JPRNT=-2,MAVISP=1,XM(1)=1.0,NJPRNT=7,
HI=0.01,HMIN=0.01,HMAX=0.01,

END

ETRANS

MP=200,

END

EMOC

EXITPL=.FALSE.,EPW=0.05,

END

EBLM

IHFLAG=0,NTQW=19,
TQW=1260.0,1260.0,1260.0,2770.0,3330.0,3960.0,4050.0,

1149.34,958.00,863.83,635.66,548.76,577.38,
 565.98,559.23,551.66,550.73,543.98,538.47,
 XTQW= -13.0,-6.0,-2.26,-2.14,-1.57,-0.89,0.0,
 1.8722,3.06,4.406,8.4344,13.9624,
 23.6164,32.6124,40.3644,50.2504,62.4584,77.9624,95.7704,
 APROF=30.,200.,400.0,1009.0,NPROF=4,KDTPLT=1, NTR=800,
 KMTPLT=1,KTWPLT=1,XSEG=-14.0,10.0,33.0,56.0,79.0,101.23,NSEGS=5,
 XINO(1)=-14.0,-12.0,-10.0,-8.0,-6.0,-4.0,
 RINO(1)=2.054,2.054,2.054,2.054,2.054,2.054,
 UEO(1)=80.0,213.0,346.0,480.0,613.0,746.0,
 TEO(1)=5709.6,5709.0,5707.5,5706.0,5704.0,5702.2,
 PEO(1)=355.2,355.0,354.3,353.65,352.9,352.0,
 &END

Input for Reading 121

LOW T CPHS

H		2		
100.	4.968			1
200.	4.968			2
H2		2		
100.	6.729			1
200.	6.560			2
H2O		2		
100.	7.961			1
200.	7.969			2
O		2		
100.	5.665			1
200.	5.433			2
OH		2		
100.	7.798			1
200.	7.356			2
O2		2		
100.	6.956			1
200.	6.961			2

END LOW T CPHS

TITLE HIGH E NOZZLE STUDY: E=1000 AND READING = 121

DATA

&DATA

ODE=1,ODK=1,TDK=1,BLM=1,IRPEAT=2,IOFF=6,
 RSI=0.5,ASUB=3.,1.5,NASUB=2,IRSTRT=0,
 ASUP=1.5,2.0,30.0,200.0,400.0,600.0,1024.0,NASUP=7,
 ECRAT=4.223,RI=2.,THETAI=25.,RWTU=2.,
 ICTYPE=0,IWALL=4,RWTD=0.4,THETA=39.41,
 THE=7.94,NWS=36,

RS= 0.0000, 1.1316, 1.1780, 1.2748,
 1.3704, 1.4198, 1.7658, 2.0876,
 2.4916, 3.0372, 5.2522, 5.7028,
 6.5606, 7.0420, 7.5072, 8.0464,
 9.0636, 9.5394, 10.6852, 12.0244,
 12.7284, 14.0056, 15.2408, 15.9610,
 16.6554, 17.3210, 18.7560, 19.6768, 20.5562,
 21.6918, 23.7554, 24.6744, 27.0428,
 29.1286, 30.1862, 32.0156,
 ZS= 0.0000, 0.3094, 0.3654, 0.4778,
 0.5908, 0.6480, 1.0430, 1.4050,
 1.8722, 2.5246, 5.5320, 6.2150,
 7.5802, 8.3862, 9.1920, 10.1592,
 12.0810, 13.0230, 15.4056, 18.4006,
 20.0684, 23.2606, 26.5588, 28.5824,
 30.6060, 32.6136, 37.1806, 40.2916, 43.4026,
 47.6334, 55.9914, 60.0166, 71.3698,
 82.7063, 89.0425, 101.2383,

&END

REACTANTS

H 2.	00	100.	G295.00	F
O 2.	00	100.	G288.30	O

NAMELISTS

```

CODE
RKT=T,P=360.0,PSIA=T,OF=T,OFSKED=5.11,
SUPAR=30.0,200.0,400.0,600.0,1024.0,ECRAT=4.223,
&END
REACTIONS
H + OH = H2O , A=8.4E21 , N=2.0 , B=0. , (AR) BAULCH 72 (A) 1OU
O + H = OH , A=3.62E18 , N=1. , B=0. , (AR) JENSEN 78 (B) 3OU
O + O = O2 , A=1.9E13 , N=0. , B=-1.79 , (AR) BAULCH 76 (A) 1OU
H + H = H2 , A=6.4E17 , N=1. , B=0. , (AR) BAULCH 72 (A) 3OU
END TBR REAX
H2 + OH = H2O + H , A=2.20E13 , N=0.00 , B=5.15 , BAULCH 72 (A) 2U
OH + OH = H2O + O , A=6.30E12 , N=0.00 , B= 1.09 , BAULCH 72 (A) 3U
H2 + O = H + OH , A=1.80E10 , N=-1. , B=8.9 , BAULCH 72 (A) 1.5U
O2 + H = O + OH , A=2.2E14 , N=0. , B=16.8 , BAULCH 72 (A) 1.5U
LAST REAX
THIRD BODY REAX RATE RATIOS
SPECIES H2,5.,5.,5.,4.,
SPECIES H2O,17.,5.,5.,10.,
SPECIES O2,6.,5.,11.,1.5,
SPECIES H,12.5,12.5,12.5,25.,
SPECIES O,12.5,12.5,12.5,25.,
SPECIES OH,12.5,12.5,12.5,25.,
LAST CARD
&ODK
EP=0.0,JPRNT=-2,MAVISP=1,XM(1)=1.0,NJPRNT=7,
HI=0.01,HMIN=0.01,HMAX=0.01,
&END
&TRANS
MP=200,
&END
&MOC
EXITPL=.FALSE.,EPW=0.05,
&END
&BLM
IHFLAG=0,NTQW=19,
TQW=1260.0,1260.0,1260.0,2770.0,3330.0,3960.0,4050.0,
1057.56,922.32,873.83,641.26,598.97,572.43,
563.59,558.51,552.33,545.82,542.90,537.82,
XTQW= -13.0,-6.0,-2.26,-2.14,-1.57,-0.89,0.0,
1.8722,3.06,4.406,8.4344,13.9624,
23.6164,32.6124,40.3644,50.2504,62.4584,77.9624,95.7704,
APROF=30.,200.,400.0,1009.0,NPROF=4,KDTPLT=1,
KMTPLT=1,KTWPLT=1,XSEG=-14.0,10.0,33.0,56.0,79.0,101.23,NSEGS=5,
XINO(1)=-14.0,-12.0,-10.0,-8.0,-6.0,-4.0,
RINO(1)=2.054,2.054,2.054,2.054,2.054,2.054,
UEO(1)=81.0,216.0,351.0,486.0,621.0,757.0,
TEO(1)=5614.0,5612.6,5610.4,5608.2,5607.0,5605.8,
PEO(1)=360.0,359.6,358.3,357.65,356.0,355.9,
NTR=800,
&END
/EOF

```

Input for Reading 137

```

LOW T CPHS
H          2
100.      4.968      1
200.      4.968      2
H2         2
100.      6.729      1
200.      6.560      2
H2O        2
100.      7.961      1
200.      7.969      2
O           2
100.      5.665      1
200.      5.433      2
OH          2
100.      7.798      1

```

200. 7.356 2
O2
100. 6.956 1
200. 6.961 2

END LOW T CPHS

TITLE HIGH E NOZZLE STUDY: E=1000 TRUNCATED TO 400:1 AND READING = 137

DATA

EDATA

ODE=1,ODK=1,TDK=1,BLM=1,IRPEAT=2,
RSI=0.5,ASUB=3.,1.5,NASUB=2,IOFF=6,IRSTRT=2,
ASUP=1.5,2.0,30.0,200.0,430.0,NASUP=5,
ECRAT=4.223,RI=2.,THETA=25.,RWTU=2.,
ITYPE=0,IWALL=4,RWTD=0.4,THETA=39.41,
THE=15.5,NWS=28,

RS= 0.0000, 1.1104, 1.1542, 1.2510,
1.2986, 1.3462, 1.4446, 1.5226,
2.7434, 3.3786, 4.7164, 5.5916,
6.0724, 6.8034, 7.2766, 7.7792,
9.3032, 9.7722, 11.0168, 11.6616,
13.7082, 14.2982, 14.8704, 16.3112,
17.6454, 19.2220, 20.1216, 20.8512,

ZS= 0.0000, 0.2814, 0.3374, 0.4496,
0.5058, 0.5620, 0.6766, 0.7662,
2.1694, 2.9508, 4.7504, 6.0442,
6.7924, 7.9832, 8.7892, 9.6756,
12.5520, 13.4938, 16.1258, 17.5666,
22.4984, 24.0228, 25.5472, 29.5942,
33.6174, 38.7360, 41.8470, 44.4864,

END

REACTANTS

H 2.	00	100.	G291.20	F
O 2.	00	100.	G285.00	O

NAMELISTS

CODE

RKT=T,P=356.8,PSIA=T,OF=T,OFKED=4.29,
SUPAR=30.0,200.0,430.0,ECRAT=4.223,

END

REACTIONS

H + OH = H2O , A=8.4E21 , N=2.0 , B=0., (AR) BAULCH 72 (A) 10U
O + H = OH , A=3.62E18 , N=1. , B=0., (AR) JENSEN 78 (B) 30U
O + O = O2 , A=1.9E13 , N=0. , B=-1.79, (AR) BAULCH 76 (A) 10U
H + H = H2 , A=6.4E17 , N=1. , B=0., (AR) BAULCH 72 (A) 30U

END TRR REAX

H2 + OH = H2O + H , A=2.20E13, N=0.00, B=5.15, BAULCH 72 (A) 2U
OH + OH = H2O + O , A=6.30E12, N=0.00, B=1.09, BAULCH 72 (A) 3U
H2 + O = H + OH , A=1.80E10, N=-1. , B=8.9, BAULCH 72 (A) 1.5U
O2 + H = O + OH , A=2.2E14 , N=0. , B=16.8, BAULCH 72 (A) 1.5U

LAST REAX

THIRD BODY REAX RATE RATIOS

SPECIES H2,5.,5.,5.,4.,
SPECIES H2O,17.,5.,5.,10.,
SPECIES O2,6.,5.,11.,1.5,
SPECIES H,12.5,12.5,12.5,25.,
SPECIES O,12.5,12.5,12.5,25.,
SPECIES OH,12.5,12.5,12.5,25.,

LAST CARD

EDOK

EP= 10.0,MAVISP=1,XM(1)=1.0,JPRNT=-2,
HI=0.010,HMIN=0.010,HMAX=0.010,ARPRNT(1)=434.0,NJPRNT=1,

END

ETRANS

MP=200,

END

EMOC

EXITPL=.FALSE.,EPW=0.05,

END

EBLM

IHFLAG=0,NTQW=15,

TQW= 1260.0,1260.0,1260.0,2700.0,3330.0,3960.0,4050.0,
1149.34,958.00,863.83,635.66,548.76,577.38,565.98,
559.23,

XTQW= -13.0, -6.0, -2.26, -2.14, -1.57, -0.89, 0.0,
 1.8722, 3.06, 4.406, 8.4344, 13.9624,
 23.6164, 32.6124, 40.3644,
 APROF=30., 200., 396.0, NPROF=3, KDTPLT=1, NTR=800,
 KMTPLT=1, KTWPLT=1, XSEG=-14.0, -2.0, 10.0, 22.0, 34.0, 44.2, NSEGS=5,
 XINO=-14.0, -12.0, -10.0, -8.0, -6.0, -4.0,
 RINO=2.054, 2.054, 2.054, 2.054, 2.054, 2.054,
 UEO= 85.0, 227.0, 368.0, 510.0, 652.0, 793.0,
 PEO= 356.4, 355.7, 355.0, 354.3, 353.6, 352.9,
 TEO= 5702.0, 5699.6, 5698.5, 5697.2, 5695.9, 5695.6,
 &END

Appendix B Pressure Integration Calculation

Pressure Integration Procedure

The force acting on the surface of a rocket nozzle can be represented as the result of normal and tangential forces. The normal force per unit area is defined as pressure. Conversely, tangential force per unit area is termed shear stress. For symmetric nozzles, only the axially directed force is of concern with regard to thrust.

According to boundary-layer theory, the normal forces acting on a rocket nozzle are independent of tangential forces (except for minor boundary-layer displacement corrections). As such, it is possible to experimentally distinguish inviscid (normal) forces from shear forces. The inviscid thrust between discrete nozzle area ratios can be determined by integrating pressure with respect to the normal surface area:

$$\Delta \text{Thrust} = \int_{A_{N_1}}^{A_{N_2}} P_w dA_N \quad (1)$$

where

P_w static wall pressure
 A_N normal surface area

or, in terms of thrust coefficient and area ratio,

$$\Delta C_{F,V} = \int_{\epsilon_1}^{\epsilon_2} \left(\frac{P_w}{P_{c,e}} \right) d\epsilon \quad (2)$$

where

$C_{F,V}$ vacuum thrust coefficient
 ϵ area ratio
 $P_{c,e}$ effective chamber pressure

Furthermore, the net gain in thrust (or thrust coefficient) between area ratios can be determined by testing a nozzle contour truncated at various area ratios. The difference

between the inviscid and net thrust (or thrust coefficient) is then the shear, or drag, decrement.

The integration of equation (2) was carried out by performing a piecewise integration of measured pressures. The relationship between pressure and area ratio was assumed to have the form

$$\frac{P_w}{P_{c,e}} = a\epsilon^b$$

This form is considered accurate due to the nearly linear nature of the pressure versus area ratio plot when shown on log-log scales (figs. 9 and 10). Coefficients a and b are determined from measurements of pressure at two distinct area ratios. Usually these points represent the two end points in the piecewise integration. The exception to this rule is the interpolation done at the lowest area ratios and the extrapolation performed out to the exit area ratio.

Determination of Inviscid Thrust Gain

As previously discussed, the thrust gain of a rocket engine between two given area ratios is the net result of the inviscid thrust gain and the drag decrement. Only the axial thrust is of concern as radial components of thrust are assumed to cancel. To determine the force of the rocket engine as the result of normal stresses (pressure), one considers only the normal component of the nozzle surface area, or

$$\Delta \text{Thrust} = \int_{A_{N_1}}^{A_{N_2}} P_w dA_N \quad (1)$$

and, since throat area A_t is constant,

$$dA_N = A_t d\epsilon$$

Also, by definition

$$\Delta C_{F,V} = \frac{\Delta \text{Thrust}}{P_{c,e} A_t}$$

Therefore,

$$\Delta C_{F,V} = \int_{\epsilon_1}^{\epsilon_2} \left(\frac{P_w}{P_{c,e}} \right) d\epsilon \quad (2)$$

As discussed previously, the plot of pressure ratio versus area ratio is nearly linear when presented on log-log scales. Therefore, since equations of the form $y = a(x^b)$ appear as straight lines on log-log paper, this relation was assumed; that is,

$$\frac{P_w}{P_{c,e}} = a\epsilon^b$$

Piecewise integration of equation (2) is then

$$\Delta C_{F,V} = \frac{a\epsilon^{b+1}}{b+1} \Big|_{\epsilon_1}^{\epsilon_2}$$

The constants a and b are determined by using two data points of pressure and area ratio, where

$$b = \frac{\ln\left(\frac{P_{w1}}{P_{w2}}\right)}{\ln\left(\frac{\epsilon_1}{\epsilon_2}\right)}$$

and

$$a = \frac{\left(\frac{P_{w1}}{P_{c,e}}\right)}{\left(\epsilon_1^b\right)}$$

Table IV shows a sample calculation of the inviscid thrust gain.

TABLE IV.—SAMPLE CALCULATION
[Nozzle contour, 1000:1; area ratio, 1030; mixture ratio, 3.84.]

Area ratio	Pressure ratio, $P_w/P_{c,e}$	Integration region	Parameter		Vacuum thrust coefficient, $C_{F,V}$
			a	b	
388.01	0.0002294	427.50 to 499.97	0.54749	-1.304734	0.01186
499.97	.0001648	499.97 to 635.04	.47666	-1.282441	.01905
635.04	.0001213	635.04 to 799.98	1.7719	-1.485888	.01682
799.98	.0000861	799.98 to 974.94	.02019	-.816495	.01387
974.94	.0000732	974.94 to 1025.0	*.02019	*-.816495	.00359
				Total	.06519

*Indicates extrapolated value.

Integration Uncertainty

The uncertainty in performing piecewise integration was examined. This was done by using the TDK program. The pressure output, at area ratios corresponding (approximately) to those at which the experimental pressure measurements were taken, was tabulated. The incremental thrust coefficient gain from area ratios of 427.5 to 1030 was predicted at 0.0600 by using the integration procedure described previously. This compares with the computationally predicted gain of 0.0610. Therefore, it seems reasonable to conclude that the accuracy of the integration procedure is within 2 percent of the actual conditions.

References

1. JANNAF Rocket Engine Performance Prediction and Evaluation Manual. CPIA-PUBL-246, Chemical Propulsion Information Agency, 1975.
2. Nickerson, G.R.; Coats, D.E.; and Dang, L.D.: Engineering and Programming Manual: Two-Dimensional Kinetic Reference Computer Program (TDK). (SN-63, Software Engineering Associates; NASA Contract NAS8-35931) NASA CR-178628, 1985.
3. Pavli, A.J.; Kacynski, K.J.; and Smith, T.A.: Experimental Thrust Performance of a High Area Ratio Rocket Nozzle. NASA TP-2720, 1987.
4. Nickerson, G.R.: The Rao Method Optimum Nozzle Contour Program, Software and Engineering Associates Inc., Carson City, NV, SEA Report No. 6/82/800.1, June 1982.
5. Evans, R.M.: Boundary Layer Integral Matrix Procedure—User's Manual. (AEROTHERM-UM-75-64, Aerotherm Acurex Corp.; NASA Contract NAS8-30930) NASA CR-144046, 1975.
6. Keller, H.B.; and Cebeci, T.: Accurate Numerical Methods for Boundary-Layer Flows. II: Two-Dimensional Turbulent Flows. AIAA J., vol. 10, no. 9, Sept. 1972, p. 1193-1199.
7. Cebeci, T.; and Smith, A.M.O.: Analysis of Turbulent Boundary Layers, Academic Press, 1974.
8. Kacynski, K.J.; Pavli, A.J.; and Smith, T.A.: Experimental Evaluation of Heat Transfer on a 1030:1 Area Ratio Nozzle. NASA TP-2726, 1987.
9. Powell, W.B.: Simplified Procedures for Correlation of Experimentally Measured and Predicted Thrust Chamber Performance. (JPL TM-33-548, Jet Propulsion Lab; NASA Contract NAS7-100) NASA CR-131519, 1973, p. 40.

1. Report No. NASA TP-2725		2. Government Accession No.		3. Recipient's Catalog No.	
4. Title and Subtitle Comparison of Theoretical and Experimental Thrust Performance of a 1030:1 Area Ratio Rocket Nozzle at a Chamber Pressure of 2413 kN/m ² (350 psia)				5. Report Date August 1987	
				6. Performing Organization Code 506-42-21	
7. Author(s) Tamara A. Smith, Albert J. Pavli, and Kenneth J. Kacynski				8. Performing Organization Report No. E-3523	
				10. Work Unit No.	
9. Performing Organization Name and Address National Aeronautics and Space Administration Lewis Research Center Cleveland, Ohio 44135				11. Contract or Grant No.	
				13. Type of Report and Period Covered Technical Paper	
12. Sponsoring Agency Name and Address National Aeronautics and Space Administration Washington, D.C. 20546				14. Sponsoring Agency Code	
15. Supplementary Notes Prepared for the 23rd Joint Propulsion Conference cosponsored by the AIAA, SAE, ASME, and ASEE, San Diego, California, June 29-July 2, 1987. AIAA report number, AIAA-87-2069.					
16. Abstract The Joint Army, Navy, NASA, Air Force (JANNAF) rocket engine performance prediction procedure is based on the use of various reference computer programs. One of the reference programs for nozzle analysis is the Two-Dimensional Kinetics (TDK) Program. The purpose of this report is to calibrate the JANNAF procedure that has been incorporated into the December 1984 version of the TDK program for the high-area-ratio rocket engine regime. The calibration was accomplished by modeling the performance of a 1030:1 rocket nozzle tested at NASA Lewis Research Center. A detailed description of the experimental test conditions and TDK input parameters is given. The results indicate that the computer code predicts delivered vacuum specific impulse to within 0.12 to 1.9 percent of the experimental data. Vacuum thrust coefficient predictions were within ± 1.3 percent of experimental results. Predictions of wall static pressure were within approximately ± 5 percent of the measured values. An experimental value for inviscid thrust was obtained for the nozzle extension between area ratios of 427.5 and 1030 by using an integration of the measured wall static pressures. Subtracting the measured thrust gain produced by the nozzle between area ratios of 427.5 and 1030 from the inviscid thrust gain yielded experimental drag decrements of 10.85 and 27.00 N (2.44 and 6.07 lb) for mixture ratios of 3.04 and 4.29, respectively. These values correspond to 0.45 and 1.11 percent of the total vacuum thrust. At a mixture ratio of 4.29, the TDK predicted drag decrement was 16.59 N (3.73 lb), or 0.71 percent of the predicted total vacuum thrust.					
17. Key Words (Suggested by Author(s)) High-area-ratio rocket Nozzle designs Rocket nozzles			18. Distribution Statement Unclassified-unlimited STAR Category 20		
19. Security Classif. (of this report) Unclassified		20. Security Classif. (of this page) Unclassified		21. No of pages 23	22. Price* A02